Barrier penetration theory in more than one dimension

Peter Ring,[a] John O. Rasmussen, and Herbert Massmann[b]

Lawrence Berkeley Laboratory, University of California Berkeley, California 94720
Fiz. Elem. Chastits At. Yadra 7, 916–951 (October–December 1976)

Quantum-mechanical tunneling theory in more than one dimension is reviewed. Several systems from nuclear and molecular science are considered specifically, such as, alpha decay of spheroidal nuclei, spontaneous fission, and reactive collinear collisions of hydrogen atoms with hydrogen molecules. The ranges of validity of various approximations that reduce to one-dimensional path integrals or Fröman-Nosov matrices are examined, testing where possible against fully quantum-mechanical coupled-channel solutions. The classical-equations-of-motion methods using complex variables (uniform semiclassical approximation) are explored for nonseparable fission-like model systems. Effects of variable valley widths, curving valleys, and of variable inertial tensors are delineated.

PACS numbers: 03.65.Ge, 24.10.Dp, 24.80.+y, 23.60.+e

INTRODUCTION

The problem of quantum-mechanical penetration of a two or more dimensional barrier occurs in a number of interesting physical situations. In this article we will review only a few situations, namely the ones which display the barrier penetration in the simplest and most explicit way.

The α-particle penetration problem is considered and several approaches are discussed. In addition we will deal with the barrier penetration in the spontaneous-fission problem. The various approximate treatments that have been used for this problem are described, including a recent barrier-model system for which a comparison of several of these methods is made. In the realm of molecular reactions, only the electron and the hydrogen nucleus have sufficiently low mass to undergo significant tunneling and we consider one of these problems, the collinear collision of a proton on a hydrogen molecule. This problem has been of much interest to molecular theorists. In all these examples we will, however, only consider the cases where the energy of the system is not too close to the top of the barrier.

Another place in nuclear physics where a tunneling process is involved is the tunneling of a nucleon or a few nucleons in stripping and pickup reactions. In the old semiclassical transfer theory of Breit and Ebel, [1] tunneling is displayed rather explicitly, but the more sophisticated modern versions of semiclassical transfer theory (K. Alder *et al.* [2] and R. Broglia and Aa. Winther[3]) don't show the tunneling in a simple way and we will therefore not discuss it in this paper. Electron tunneling which enters in a rather complicated way in the electron capture and loss problems from ions moving through matter also is not considered here. A review of the early quantum-mechanical treatments of this subject by Oppenheimer[4] and Brinkman and Kramers[5] has been given by Raisbeck and Yiou. [6]

The main object of this paper will be to present the various methods used in solving the multidimensional barrier-tunneling problem. The coordinates orthogonal to the barrier-penetration coordinate and the effect of a coordinate-dependent inertial tensor will be considered and an attempt will be made to isolate these different components of the problem.

1. MULTIDIMENSIONAL BARRIER PENETRATION IN ALPHA DECAY

Examination of detailed methods for two-dimensional barrier problems. We now consider in more detail the penetrability problem for anisotropic barriers in alpha decay. Beyond the range of nuclear forces we have the simple Hamiltonian for a spin-zero system

$$H=-\frac{\hbar^2}{2\mu}\nabla^2-\frac{\hbar^2}{2\mathcal{I}}J_{\theta_i}^2+\frac{2Ze^2}{r}+\frac{2e^2Q_0}{2r^3}P_2(\cos\gamma), \tag{1}$$

where the ∇^2 Laplacian operates on the coordinates of the alpha in the lab-fixed system θ, ψ, with r the center-to-center separation distance, μ the reduced mass $Mm_\alpha/M+m_\alpha$, $\mathcal{I}$ the nuclear moment of inertia, $J_{\theta_i}^2$ the square of the nuclear rotational-angular-momentum operator operating on the Eulerian angles θ_i defining the nuclear symmetry axes in the lab frame, Z is the charge and Q_0 the intrinsic quadrupole moment of the daughter nucleus, and γ is the angle between the alpha direction (θ,ψ) and the nuclear symmetry axis (θ_1,θ_2). The problem reduces to a two-dimensional one in r and γ when transformed to the body-fixed coordinate system (see Rasmussen and Segall[7]). The wave equation is transformed to a set of coupled-channel second-order radial equations by expanding the wave function as follows:

$$\Psi=\sum_{l_{\text{even}}}\frac{u_l(r)}{r}\sum_m(llm-m\,|\,00)Y_{lm}(\theta,\psi)\sqrt{\frac{2l+1}{8\pi^2}}D^l_{-m0}(\theta_i) \tag{2}$$

Left-multiplying the wave equation $(H-E)\Psi=0$ by the complex conjugate of an angular function

$$\sum_{m'}(l'l'm'-m'\,|\,00)Y^*_{l'm'}(\theta,\psi)\sqrt{\frac{2l'+1}{8\pi^2}}D^{l'*}_{-m'0}(\theta_i)$$

and integrating over all angular space θ, ψ, and θ_i gives the set of coupled-channel equations.

$$-\frac{\hbar^2}{2\mu}\frac{d^2u_{l'}}{dr^2}+\left[\frac{2Z^2}{r}+\left(\frac{\hbar^2}{2\mu r^2}+\frac{\hbar^2}{2\mathcal{I}}\right)l'(l'+1)-E\right]u_{l'}$$
$$+\frac{Q_0e^2}{r^3}\sum_l u_l\langle l'l',\,0\,|\,P_2(\cos\gamma)\,|\,ll,\,0\rangle=0. \tag{3}$$

In the total-spin-zero case (as for even-even ground-state alpha decay) the matrix elements in (3) have the simple form first given by Racah[8]

[a] Present address: Physics Department, Technische Universität München, West Germany.

[b] Present address: Faculty of Science, University of Chile, Santiago, Chile.

$$\langle l'I', 0 | P_2 | lI, 0\rangle = \frac{1}{5}\sqrt{(2l+1)(2l'+1)}(ll'00|20)^2$$

The numerical solution of the problem for alpha decay usually involves application of some double-ended boundary conditions. At the nuclear surface or on a spherical surface R_s nearby one seeks the irregular solutions for all components u_l. That is, all solutions should be exponentially decreasing solutions appropriate to the quasibound alpha state in the parent nucleus. At large distance the wave functions will be oscillatory, and often one imposes the experimental relative intensities of decay to various rotational states. In practice one cannot carry through the outward integrations, since the exponentially decreasing solutions are not stable, and any rounding errors in the integration routine will grow exponentially. Thus, one resorts to inward integrations from some large distance beyond which the quadrupole-potential term is negligible. If one takes N equations, one obtains a complete linearly independent set of $2N$ solutions by successively matching at large r each channel solution u_l and its derivative to the irregular Coulomb solution $G_l(\eta, \rho)$ and then the regular $F_l(\eta, \rho)$. The values of these wave functions at R_s make up the real (for G_l initial) and imaginary (for F_l initial) components of an $N\times N$ matrix, A. The inverse A^{-1} of this matrix when operating on the column vector $u_l(R)$ gives the amplitudes (and phases relative to pure Coulomb waves) in the asymptotic region. The alpha intensities are the squares of amplitudes times the velocity of the alpha group. The matrix is usually factored into a diagonal matrix P, whose elements $P_{ll}^{1/2}$ are the square roots of JWKB penetration factors for each channel in the absence of the quadrupole term in the Hamiltonian (1) and an $N\times N$ matrix K:

$$A^{-1} = PK$$

The matrix K is usually called the Fröman matrix,[9] and it goes over to a unit matrix as $Q_0 \to 0$.

An example of the K matrix is shown below for coupled-channel integration for ^{242}Cm alpha decay[10]:

$$K = \begin{pmatrix} 1.015+0.0116i & -0.1674-0.0176i & 0.01166+0.00217i & (-5.09-1.3i)10^{-4} \\ -0.2107-0.0456i & 0.954-0.00158i & -0.120-0.00592i & (7.26+0.679i)10^{-3} \\ 0.02114+0.0135i & -0.190-0.0595i & 0.919-0.0036i & -0.101-0.00187i \\ -0.00109-0.00216i & 0.0189+0.0187i & -0.205-0.0893i & 0.909-0.0241i \end{pmatrix}.$$

where the successive elements refer to $l=0, 2, 4, 6$. The P matrix in this case has elements $p_{00}=1.30\cdot10^{-27}$, $p_{22}=4.67\cdot10^{-28}$, $p_{44}=4.21\cdot10^{-29}$, $p_{66}=9.30\cdot10^{-31}$. Because of the off-diagonal elements in the K matrix, a wave function that is purely one l value on the surface at R has admixed various l values at large distances outside the barrier. Sometimes the K matrix is constructed so as to transform the Legendre expansion of the wave function on a spheroidal surface, a constant nuclear-density surface or a Nilsson stretched-coordinate surface,[11] rather than the spherical surface expansion of our numerical example. One may refer to the literature for examples in which spheroidal coordinates are used.[7,12]

It may at first glance seem puzzling that the K-matrix given above has alternating signs for its elements, while the analogous matrix of Fröman[9] has all elements with the same sign. In both cases the nucleus was considered prolate. However, the K-matrix above transforms the Legendre expansion on a spherical surface, while Fröman's matrix transforms the Legendre expansion on the spheroidal nuclear surface. The wave propagation from the spherical surface is more favorable in the equatorial region, since the quadrupole term makes the barrier lower in the equatorial region for a given radius. On the other hand, for wave propagation from the spheroidal nuclear surface, the polar regions are favored. The greater distance from the center at the poles means the lower net potential barrier is at the poles, and furthermore the barrier is thinnest in the polar regions.

Coupled-channel calculations have also been made[13] for odd-mass nuclei, such as ^{253}Es and ^{255}Fm, where the calculated K-matrix is a 9×9, including the lowest five members of the favored rotational band and all $l=0, 2$, and 4 waves.

Let us now examine Fröman's approximation. It is most accurate in the case of vanishing nuclear rotational energies (infinite moment of inertial), so we consider that case. In his method Fröman carries out an Legendre expansion of the wave function on the interior surface, as in the coupled-channel method. For each Legendre component on the surface one propagates the wave function out to large distance by one-dimensional path integrals at constant polar angle γ taking into account the potential-energy terms of the Hamiltonian.

By use of the JWKB approximation a particular l component on the interior surface is transformed from $Y_{l0}(\gamma, \psi)$ at R_k to

$$Y_{l_0}(\gamma, \psi)\exp\left\{-\frac{1}{\hbar}\int_{R_s(\gamma)}^{r_t(\gamma)}\sqrt{2\mu\,(V(\gamma, r)-E)}\,dr\right\}, \tag{4}$$

where

$$V(\gamma, r) = \frac{2Ze^2}{r} + \frac{Q_0e^2}{r^3}P_2(\cos\gamma), \tag{5}$$

and $r_t(\gamma)$ is the outer classical turning distance. The wave function outside the barrier is re-expanded in Legendre functions. When the expansion coefficients are divided by the penetration factor for no quadrupole distortion of shape or field one has the elements $k_{ll'}$ of the Fröman matrix K. Let us write out these relations explicitly

$$k_{ll'} = \int\int Y_{l'0}^{*}\exp\left\{-\frac{1}{\hbar}\int_{R_s(\gamma)}^{r_t(\gamma)}\sqrt{2\mu\,(V(r, \gamma)-E)}\,dr + \frac{1}{\hbar}\int_{R_0}^{r_t}\sqrt{2\mu\,(V_c-E)}\,dr\right\}Y_{l0}\,d\omega, \tag{6}$$

with

$$V_c = 2Ze^2/r. \tag{7}$$

To further simplify, Fröman expands the integrand (under the assumption that the quadrupole term is small):

$$\sqrt{V(r,\gamma)-E} \approx \sqrt{V_c-E}\,(1+(Q_0e^2/r^3)\,P_2(\cos\gamma)/[2(V_c-E)]+\ldots).$$

The argument of the exponent then goes over to

$$-P_2(\cos\gamma)\frac{\sqrt{2\mu}}{\hbar}\int_{R_s}^{r_t}\frac{1}{2}\frac{Q_0e^2}{r^3\sqrt{V_c-E}}\,dr = -BP_2(\cos\gamma),$$

defining the argument B of the Fröman matrix. Thus equation (6) can be approximately written

$$k_{ll}^{(\beta)} = \int\int Y_{l'0}^{*}\exp\{-BP_2(\cos\gamma)\}\,Y_{l0}\,d\omega. \tag{8}$$

We shall not work out here the analytical expression for the Fröman argument B appropriate to the K-matrix from a spherical surface. Rather, we quote Fröman's expression for the transformation from a spheroid

$$B = \chi\beta_2\sqrt{[5KR_0/(4\pi\chi)]\,(1-KR_0/\chi)}\,[4/5-(2/5)\,(KR_0/\chi)], \tag{9}$$

where $\chi = 4Ze^2/\hbar v$ is twice the Sommerfeld parameter η and K is the wave number. We have specialized Fröman's formula for the usual case of a uniformly charged spheroid. The parameter β_2 is the usual coefficient of Y_{20} in the expansion of the nuclear shape.

Nosov,[14] independently of Fröman and working from an equation of Strutinsky,[15] arrived at a matrix-element expression similar to Eq. (9). His expression becomes, using Fröman's notation,

$$B = \chi\beta_2\sqrt{\frac{5}{4\pi}}\left[\sqrt{\frac{KR_0}{\chi}\left(1-\frac{KR_0}{\chi}\right)}\,\frac{4}{5}-i\,\frac{2}{5}\frac{K^2R_0}{\chi}\right]. \tag{10}$$

The important new aspect in Nosov's expression is the imaginary component, representing the Coulomb excitation. The real parts agree in the leading term of Fröman's expression.

Yet another approximation to the problem was applied by Chasman and Rasmussen,[16] taking approximate radial wave functions for $(\alpha_l+\beta_l r^{-3/2})G_l(r)$ within the barrier and choosing constants α_l and β_l to optimize solutions in the presence of the quadrupole-potential term. The transmission matrix obtained in this way also compares favorably with the exact solutions.

2. MULTIDIMENSIONAL BARRIER PENETRATION AND FISSION

Introduction

Another field in nuclear physics where a multidimensional barrier penetration manifests itself is in the study of spontaneous and induced fission. Presently nearly all the fission barriers are calculated by a macroscopic-microscopic method. In this method the smooth trends of the potential energy (with respect to particle numbers and deformation) are taken from a macroscopic model, the liquid-drop model, and the local fluctuations, also called shell corrections, are taken from a microscopic model. We shall not try to review the early attempts to calculate theoretically the fission-barrier penetrability, for prior to the Strutinsky[17] method of applying the shell corrections to the liquid-drop potential surfaces, the fission-barrier heights and shapes were simply not at all understood. Several groups[18–24] have since then made careful application of the Strutinsky method and now we can have confidence that the main aspects of the potential landscape along the fission trajectories are well known. In the region where spontaneous fission rates are known there seems to be a two-humped barrier, with the notable fission isomerism discovered by Polikanov *et al.*,[25] involving shape-isomeric metastable states in the minimum between the two barriers. It also appears that the innermost saddle may often be unstable with respect to gamma deformation,[26] i.e., deviations from cylindrical symmetry, while the outer saddle may be unstable with respect to the reflection symmetry.[27] It would appear that the asymmetry in the fission-fragment mass distribution is derived from this instability at the second barrier.

In order to describe the deformation-energy surfaces for the fission process one needs at least two or three deformation parameters to define the nuclear shape. These generalized coordinates, which are strongly coupled, give the generalized forces acting on the fissioning nucleus. For a complete dynamical description of the fission process, however, it is not enough to have a good knowledge of the potential surface, but also a knowledge of the inertial tensor is needed in order to find out how the nucleus will react to the generalized forces. The inertial tensor, of such great importance to the barrier-penetration calculations, is only poorly known.

R. Nix[28] has carried out extensive derivations and calculations of irrotational-flow hydrodynamical inertial tensors for fission trajectories. The inertial tensor so obtained is, however, too small by a factor of approximately five, i.e., the flow during the barrier penetration is not irrotational. Now it is generally assumed that the first stage of the fission process, the penetration through the barrier, occurs adiabatically and that the cranking model can be used to evaluate the inertial tensor. The Pauli–Strutinsky group[18,29] and others[30] have extensively been exploring cranking calculations for the inertial tensor. These calculations show that the inertial tensor depends strongly on the generalized coordinates, i.e., the inertial tensor also gives a coupling between the different degrees of freedom. In the one-dimensional case however, the coordinate dependence of the inertia introduces no new difficulty since it can be transformed away. H. Hofmann and K. Dietrich[31] have shown how to transform the Schrödinger equation with variable mass $m(q)$ into one with constant mass m_0 by modifying the potential. The one-dimensional Schrödinger equation is:[1)]

$$H\Psi(q) = \left[-\frac{\hbar^2}{2}\frac{1}{\sqrt{m(q)}}\frac{d}{dq}\frac{1}{\sqrt{m(q)}}\frac{d}{dq}+V(q)\right]\Psi(q) = E\Psi(q). \tag{11}$$

Performing the following transformation

$$x(q) = \int^{q}\sqrt{m(q')/m_0}\,dq', \tag{12}$$

[1)]The general expression for the kinetic energy with variable inertia in curvilinear coordinates for many degrees of freedom has been described by H. Hofmann.[32]

where m_0 is an arbitrary constant mass, one obtains the Schrödinger equation:

$$\left[-\frac{\hbar^2}{2m_0}\frac{d^2}{dx^2}+\tilde{V}(x)\right]\tilde{\Psi}(x)=E\tilde{\Psi}(x), \tag{13}$$

where $\tilde{V}(x)=\tilde{V}(x(q))=V(q)$ and $\tilde{\Psi}(x)=\tilde{\Psi}(x(q))=\Psi(q)$. This transformation corresponds to a stretching of the potential in such a way that the mass becomes constant.

Another aspect of the fission problem, recently stressed by L. Moretto and R. P. Babinet, [33] is that, besides the coordinates describing the surface configuration, one should also consider the pairing-correlation parameters as dynamical variables.

To summarize, the fission process is a challenging multidimensional barrier-penetration problem, a problem that has been tackled by many groups introducing more or less drastic approximations. Some of these approaches we will now describe briefly.

One dimensional WKB method

The first calculations of fission lifetimes [19] after the Strutinsky prescription was introduced took into account as coordinates only ε_2 and ε_4 (that is quadrupole and hexadecupole deformations) to define the nuclear shape. In order to calculate the penetrability the problem was simplified to a one-dimensional barrier-penetration problem, constructing a path on the energy surface by minimizing the potential energy with respect to ε_4 for each ε_2 and then projecting this path onto the ε_2 axis. The penetrability was then obtained by using the one-dimensional WKB approximation:

$$P=\exp\left\{-2\int_{\varepsilon'}^{\varepsilon''}\sqrt{\frac{2B}{\hbar^2}(W(\varepsilon)-E)}\,d\varepsilon\right\}=\exp(-K). \tag{14}$$

An improved expression was shown by P. Fröman and N. Fröman [34] to be:

$$P=\{1+\exp(K)\}^{-1}. \tag{15}$$

In this early calculation the inertial mass B associated with fission was taken as a constant or was parametrized as a function of ε_2 in some simple manner. E is the initial energy of the nucleus in the fission direction and $W(\varepsilon)$ represents the barrier as obtained from the potential-energy surface just as described above. Later essentially the same type of calculations were performed by Randrup *et al.*, [35] to predict the fission half-lives of heavy elements. Here not only P_2 and P_4 distortions of the nucleus were included, but also coordinates were introduced to describe P_3 and P_5 distortions and the gamma degree of freedom.

Stationary-action path method

The next refinement in the fission-barrier-penetration problem was introduced by the Pauli–Strutinsky group; see Brack *et al.* [18] The two shape coordinates used in their calculations to describe the fissioning nucleus were a separation or elongation coordinate c and a necking-in coordinate h. Figure VIII. 4 of Ref. 18 shows a contour map of the liquid-drop energy, the energy shell corrections for neutron and protons, and the total deformation energy for ^{240}Pu. As already mentioned, these authors studied the inertial tensor within the cranking model. A contour map of the different components of the inertial tensor for ^{240}Pu is shown in Fig. IX. 4 of Ref. 18; the strong shape dependence of the inertial tensor is readily observed. The mass tensor component corresponding to the elongation coordinate generally exhibits a large maximum at the saddle. It seems likely that the fission trajectory for barrier penetration might avoid the high-inertia region by avoiding the saddle, even at the cost of a higher potential barrier. As J. Griffin [36] pointed out, if the inertial tensor has nonzero off-diagonal components or if the components depend on the coordinates, then one's intuition regarding the fission trajectory based on the potential map may be completely wrong. In other words, to assume that the fission trajectory follows along the bottom of the valley may not be adequate. In order to find the path one resorts to classical mechanics by invoking the least-action principle.

In classical mechanics the action is defined by:

$$S=\int_{t_1}^{t_2}\sum_i p_i\dot{q}_i\,dt=\int_{q_1}^{q_2}\sum_i p_i\,dq_i. \tag{16}$$

Here $\{q_i\}$ are the coordinates describing the system and $\{p_i\}$ are the corresponding canonically conjugate momenta. The principle of least action states [37,38] that in a system for which the Hamiltonian H is conserved (i. e., if $H(q,p)=E=\text{const}$) one has $\Delta S=0$ where the variation Δ does not include all the virtual displacements of the system, but only those for which the energy is conserved along the varied path. One has:

$$p_i=\frac{\partial\mathcal{L}}{\partial\dot{q}_i}=\frac{\partial}{\partial\dot{q}_i}\left(\sum_{i,j}B_{ij}(q)\dot{q}_i\dot{q}_j-W\right)=\sum_j B_{ij}(q)\frac{dq_j}{dt} \tag{17}$$

also

$$E=\frac{1}{2}\sum_{i,j}B_{ij}(q)\frac{dq_j}{dt}\frac{dq_i}{dt}+W(q), \tag{18}$$

from which dt can be found:

$$dt=\sqrt{\sum_{i,j}B_{ij}(q)\,dq_i\,dq_j}\Big/[2(E-W)]. \tag{19}$$

Substituting (19) and (17) into Eq. (16) we find

$$S=\int_{\sigma_1}^{\sigma_2}d\sigma\sqrt{2(E-W(\sigma))\sum_{i,j}B_{ij}(q)\frac{dq_i}{d\sigma}\frac{dq_j}{d\sigma}}, \tag{20}$$

where σ is some arbitrary parameter along a trajectory and B_{ij} is the inertial tensor, which may also depend on σ. During the tunneling process $W>E$, and the integrand in Eq. (20) is purely imaginary. The tunneling probability is given in the usual way by:

$$P=\left|\exp\left(\frac{iS}{\hbar}\right)\right|^2=e^{-2|S|/\hbar}. \tag{21}$$

The way Brack *et al.* [18] proceeded to find the trajectory which makes $|S|$ smallest was by forcing the trajectory through several points between the two endpoints σ_1 and σ_2. These intermediate points were then varied until the smallest action $|S|$ was obtained. The trajectory so obtained usually did not follow the steepest descent of the potential and did not lead through the extremal points of the deformation energy. It should still be noted that the entrance point (σ_1) and exit point (σ_2) in Eq. (3.11) should be determined in such a way that the action integral is also stationary against variation of these endpoints. The entrance point σ_1 is usually

chosen to lie 0.5 MeV (zero-point energy) above the bottom of the well (which is a local minimum of the total deformation energy surface); σ_2 then has to lie on the energy contour with the same energy E.

T. Ledergerber and H. C. Pauli,[30] using the same method (as the one described in Ref. 18), have done calculations using three deformation parameters: an elongation coordinate, a constriction or necking-in coordinate, and a parameter describing the left-right asymmetry. The lifetimes obtained from these calculations are in order-of-magnitude agreement with the experimental data; they also show that mass-asymmetric fission is favored and that the most probable mass division (peak-to-peak ratio) agrees with the experimental data.

In this multidimensional approach,[18,30] however, one still ignores the kinetic energy tied up in the motion orthogonal to the fission path (which may change along the path). The question of inclusion of zero-point energy for the fission degree of freedom depends on how the potential surface was derived. It has been customary in shell-corrected liquid-drop model work (Strutinsky method) to ignore all zero-point vibrational-energy corrections, since they would require assumptions about an inertial tensor. Thus, liquid-drop-model parameters are adjusted to fission-barrier heights. With such a surface it is clearly incorrect simply to add zero-point energies. This point is closely related to the point made by Maruhn and Greiner[39]; for spontaneous fission from a spheroidal ground state the number of degrees of freedom for quadrupole vibrations is three; that is, the ground state would have $(3/2)\hbar\omega$ of zero-point energy. At the saddle the frequency of the beta-vibrational mode in the fission direction has become imaginary, leaving only two units of zero-point energy, those associated with the gamma-vibrational (axial-symmetry-breaking) mode. In order to include these zero-point energy corrections (without modifying the fission-barrier heights) Maruhn and Greiner readjusted some of the liquid-drop parameters of Myers and Swiatecki[40] to lower the ground-state potential energy (and that of the final fragments) by the zero-point energy, which was obtained from the first 2^+ state experimentally observed.

Tunneling and the inverted potential energy surface

Consider a system which moves toward a barrier, and let time be the parameter in the equations of motion describing the system. If the time increments are kept real, the system will move toward the barrier and then be reflected at the barrier and move back. If however, one takes purely imaginary time increments when the system is at the turning point, the system will start tunneling. In other words, during the tunneling process, the system follows the classical equations of motion but with purely imaginary time increments. (See also Fig. 4 and the discussion below.)

If at the classical turning point of the fission degree of freedom all the other degrees of freedom are also at a turning point (or, in other words, if the system when it reaches the barrier is at rest), then the tunneling process can be visualized by a very simple picture. If the system is at rest at the turning point and if one uses purely imaginary time increments thereafter (until the tunneling is completed), then all the coordinates will remain real and all quantities related to odd powers of the time (for example velocities, momenta, angular momenta, etc.) will be purely imaginary; quantities which depend on the square of momenta (for example the kinetic energy, centrifugal force, etc.) will change sign. It is now easy to see that the system can equivalently be described by using only real time increments and changing the sign of $(V-E)$. That is, the tunneling trajectories can be obtained by finding how the system moves on the inverted potential surface.[41] For the fission example, the entrance point σ_1 will now be close to the top of a hill and the fission valley will be a mountain ridge starting somewhere close to the hill (see Fig. 1 for a simple illustration of this idea). The system now has to roll down the hill and up the mountain ridge (following the classical equations of motion) in such a way that it does not fall off the ridge to either side but reaches the exit point σ_2 where the velocity is zero again; (at this point, if one wants to follow the system into the fission valley, one would switch to the ordinary potential surface again). If after the system reaches σ_2 the time increments are kept purely imaginary (or, equivalently, using real time one keeps the inverted potential surface), the system will move toward σ_1 again. Finding the tunneling trajectory then, is equivalent to finding the periodic orbit on the inverted potential surface. In the example shown in Fig. 1 there is only one point (in general, it is a certain interval) on the entrance and one point on the exit energy contour which are connected through classical equations of motion; therefore when looking for the trajectory with the minimum action $|S|$ one also has to vary the endpoints σ_1 and σ_2 until the minimum is achieved. Another example of motion on an inverted potential surface is given in Appendix 1.

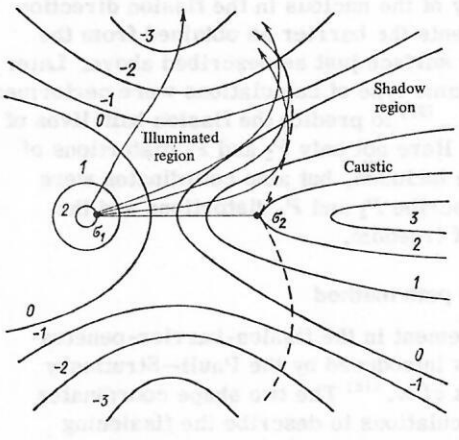

FIG. 1. Schematic representation of a contour map of a potential-energy surface turned around to study the classical motion below the barrier. The entrance and exit points, σ_1 and σ_2, lie on the same equipotential. The hill at the left side corresponds to the potential well in which the nucleus sits before fissioning, and the mountain range at the right represents the fission valley.

Quantum-mechanical DWBA approach

The two-dimensional Schrödinger equation has the form:

$$H\Psi=\Big[-\frac{\hbar^2}{2}\sum_{i,j=1,2}\frac{1}{D}\frac{\partial}{\partial q^i}Dg^{ij}\frac{\partial}{\partial q^j}+V(q^1,q^2)\Big]\Psi=E\Psi, \tag{22}$$

where g^{ij} are the contravariant components of the inertial tensor (g_{ij}) and $D=\sqrt{\det(g_{ij})}$; $V(q^1,q^2)$ is the potential energy, a function of the curvilinear coordinates q^1 and q^2.

In Appendix A of Ref. 42, H. Hofmann describes a method for finding a coordinate transformation $x=x(q^1,q^2)$, $y=y(q^1,q^2)$ which has the following properties: (i) that the off-diagonal components of the inertial tensor expressed in the new coordinates vanishes (i.e., $m_{xy}=m_{yx}=0$); (ii) that the trajectory $y=0$ defines a path of minimal potential energy (i.e., $(\partial V(x,y)/\partial y)_{y=0}=0$).

Hofmann, [42] using a transformation of coordinates like the one just described, using a harmonic approximation for the potential perpendicular to the fission path, and with the additional assumptions that the mass tensor components do not depend on the coordinate y, reduced the Hamiltonian Eq. (22) to:

$$H=-\frac{\hbar^2}{2}\Big[\frac{1}{\sqrt{m_xm_y}}\frac{\partial}{\partial x}\sqrt{\frac{m_y}{m_x}}\frac{\partial}{\partial x}+\frac{1}{m_y}\frac{\partial^2}{\partial y^2}\Big]+V(x,0)+\frac{m_y\omega^2}{2}y^2 \tag{23}$$

and solved it approximately in what can be called the first truly two-dimensional quantum-mechanical dynamical treatment of the fission process. In Eq. (23) $\omega(x)$ is defined by

$$\omega^2(x)=\frac{1}{m_y(x)}\frac{\partial^2V(x,y)}{\partial y^2}\Big|_{y=0}. \tag{24}$$

The Hamiltonian is then separated into an adiabatic part H^{ad} and a nonadiabatic H^{nad} part. If the system is initially in an oscillator state n, then $H^{\mathrm{nad}}=H-H^{\mathrm{ad}}$ can produce transitions to other oscillator states m. The probability amplitudes A_{mn} of finding the system after the barrier penetration in a state m satisfies an integral equation for which Hofmann uses the Born approximation (DWBA) to get an approximate solution. This use of the DWBA, however, as we will see later, is probably only good when considering transitions which start from the ground state before fission. When starting from an excited state, the transition probabilities to the ground state are usually higher by some orders of magnitude than the ones to excited states (even in the case where the coupling between the two degrees of freedom is quite small). The reason is that the penetrability is much higher for the case of the ground state.

Study of a fission-barrier model system

Now we will study a two-dimensional model of a fission-like barrier system. In order to investigate the full two-dimensional dynamics and to test various approximations it is of value to study a model system with the potential given by an analytical function. An example studied by Massmann *et al.* [43] takes a Hamiltonian with potential giving a Gaussian barrier in the x direction (x being the fission coordinate) and an harmonic potential in the y direction. The mass tensor was taken to be diagonal and constant; the width of the valley, however, was variable. The Hamiltonian considered was:

$$H=p_x^2/2m_x+p_y^2/2m_y+V_0\exp[-(x/a)^2]+C\{1+\alpha\exp[-(x/a)^2]\}y^2/2. \tag{25}$$

A nonzero value of the "coupling constant" α allows the width of the valley to vary over the saddle, and by doing so couples the two degrees of freedom. The numerical values were chosen to as to correspond to a typical fission case: $m_x=500\ \mathrm{MeV}^{-1}$, $V_0=7$ MeV, $m_y=4.7\ \mathrm{MeV}^{-1}$, $a=0.185$, $C=5.1$ MeV, $E_{\mathrm{tot}}=6.0$ MeV. This choice of C and m_y gives a frequency of about 1 MeV, typical of say a gamma-vibrational mode. The coordinates x and y are dimensionless and correspond for instance to the deformation parameters ε_2 and ε_4.

Exact quantum-mechanical solution

A fully two-dimensional quantum-mechanical solution of this model is possible for not too strong coupling constant α. The method is analogous to the coupled-channel calculations described for alpha-decay: One expands the two-dimensional wave-functions in a set of product wave functions:

$$\Psi^{(\mu_0)}=\sum_\nu u_\nu^{(\mu_0)}(x)\,\psi_\nu(y), \tag{26}$$

where $\{\psi_\nu\}$ is an appropriate orthonormal basis set. In this it is reasonable to choose the harmonic oscillator eigenfunctions of the y-dependent potential for $|x|\to\infty$, where the coupling term α is negligible. The index μ_0 denotes the boundary condition that in channel μ_0 one has for $x\to-\infty$ an incoming wave with unit amplitude $e^{ik_{\mu_0}x}$ and a reflected wave $r_{\mu_0}\cdot e^{-ik_{\mu_0}x}$, but in all the other channels for $|x|\to\infty$ only outgoing waves. Substituting this expansion into the wave equation:

$$(H-E)\,\Psi=0,$$

left multiplying by $\psi_\nu^*(y)$, and integrating over y from $-\infty$ to $+\infty$ gives coupled-channel equations in x:

$$\frac{d^2}{dx^2}u_\nu^{(\mu_0)}(x)=\sum_{\nu'}B_{\nu\nu'}^{(\mu_0)}(x)\,u_{\nu'}^{(\mu_0)}(x). \tag{27}$$

For $\alpha=0$ the equations will be uncoupled and the solutions are simply the product of one-dimensional wave-functions in the x and y directions. Of course, a part of the total energy, $(\mu_0+\frac{1}{2})\hbar\omega_y$, is tied up in the y-mode, and the available energy for the one-dimensional barrier penetration in the x-direction is correspondingly reduced. The matrix in Eq. (27) $B_{\mu\mu'}(x)$ is given by

$$B_{\mu\mu'}(x)=\Big\langle\psi_\mu\Big|\Big\{-\frac{m_x}{m_y}\frac{\partial^2}{\partial y^2}+\frac{2m_x}{\hbar^2}(V(x,y)-E)\Big\}\Big|\psi_{\mu'}\Big\rangle. \tag{28}$$

In order to find the solution with the correct boundary conditions, one integrates the coupled equations (Eq. 27) starting from $x\to+\infty$ with outgoing waves as initial conditions and integrating towards $x\to-\infty$. This is repeated for each channel on the right side (if the channel is closed, instead of an outgoing wave an exponentially decreasing wave is used). At the left side of the barrier one will then have incoming and outgoing waves in each channel. A matrix inversion then gives the correct linear combination of waves to be used in order to satisfy the boundary condition on the left side.

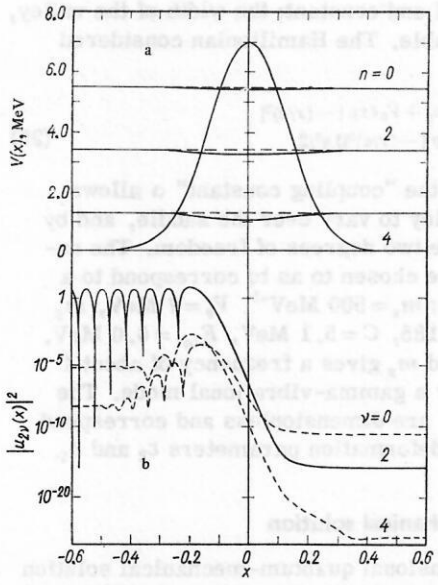

FIG. 2. Fission barrier and the square of the quantum-mechanical channel function $u_{2\nu}(x)$ for an incoming wave for the channel $\mu=2$.

Figure 2 shows in its upper part the shape of the Gaussian barrier together with the adiabatic translational energies in the x-direction for the three y-vibrational channels $n=0$, $n=2$, and $n=4$. Let's remember that the problem we are solving is typical of sub-barrier fission, with ~4.5 MeV of excitation and ~1.5 MeV below the classical barrier threshold (the coupling is $\alpha=0.1$). Higher -n channels are obviously closed, and odd-n channels are not coupled for parity reasons. The lower part of the diagram plots the square of the wave-functions for an incident wave from the left in channel $\mu=2$ (i.e., $|u_{2\nu}(x)|^2$). We note the standing wave in the channel $\mu=2$ on the left side of the barrier, as most of the flux is elastically reflected. About 10^{-5} of the total flux is inelastically reflected in channel $\mu=4$ and 10^{-8} in channel $\mu=0$. To the right of the barrier $\nu=0$, 2, and 4 waves are transmitted at the 10^{-10}, 10^{-15}, and 10^{-24} probability levels, respectively. There is a vibrational "cooling" effect[2)] on the passage through the barrier, with $\nu=0$ transmitted waves dominating regardless of the vibrational state incident on the barrier. Only in the case of α very close to zero, a constant valley width, will the "cooling" feature not appear (see Fig. 3). In a realistic fission landscape coupling is sure to be ample, both through valley-width variations and mass-tensor changes.

We may, as with alpha decay through anisotropic barriers, express the transmission alteration of amplitudes through an $N\times N$ square matrix. This matrix operating on the column vector of incident amplitudes in various vibrational states gives the final transmitted-wave amplitude matrix:

$$A^{-1}=\begin{pmatrix} 3.74\cdot10^{-3} & 9.64\cdot10^{-6} & 1.01\cdot10^{-8} \\ 9.64\cdot10^{-6} & 5.17\cdot10^{-7} & 9.93\cdot10^{-10} \\ 1.01\cdot10^{-8} & 9.93\cdot10^{-10} & 6.83\cdot10^{-12} \end{pmatrix}.$$

[2)]The "cooling" should not be interpreted in the framework of thermodynamics, since the process considered here is a completely reversible one.

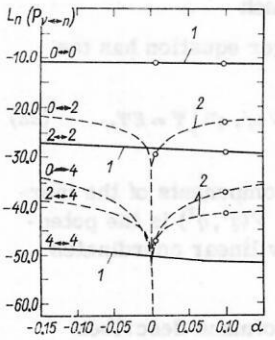

FIG. 3. Penetrabilities $P_{\mu\nu}$ for different values of the coupling constant α. The lines correspond to the QM coupled-channel calculations (1—diagonal penetrabilities; 2—nondiagonal penetrabilities) and the points correspond to the USCA calculations.

We now factor this matrix to get a matrix analogous to the Fröman matrix, that is, one which goes over to a unit matrix as the coupling α goes to zero: $A^{-1}=PK$, with P coming from the solutions of the uncoupled $\alpha=0$ problem.

$$P=\begin{pmatrix} 4.09\cdot10^{-3} & 0 & 0 \\ 0 & 7.4\cdot10^{-7} & 0 \\ 0 & 0 & 1.2\cdot10^{-11} \end{pmatrix},$$

and

$$K=\begin{pmatrix} 0.905 & 2.36\cdot10^{-3} & 2.47\cdot10^{-6} \\ 13.0 & 0.699 & 1.34\cdot10^{-3} \\ 841.0 & 82.8 & 0.569 \end{pmatrix}.$$

The K matrix in this "fission" example is so strongly unsymmetric that it would be clearly inappropriate to apply the Fröman approximation as it is used in alpha decay. This asymmetry in the K matrix evidently results from the fact that the different channel components see greatly differing barriers in the "fission" case. The transmission matrix A^{-1} itself is symmetric as the result of the symmetry of the potential in our model.

The coupled-channel code described above can take into account only a finite number of channels; it is therefore useful only for problems where one gets convergence on taking into account a reasonable number of channels. In the calculations described here, three open channels were included. Taking into account a fourth (closed) channel changed the results only in the fourth significant figure. For realistic surfaces, in order to expand the wave function Eq. (26), many more channels have to be included. This not only involves more computer time, but also closed channels with higher energy require special handling.

Quantum-mechanical adiabatic approximation

An obvious approximation to be tested by the coupled-channel solution is that the y-direction wave function, particularly the Gaussian of the zero-point lowest state, adiabatically adjusts its width as the valley changes along the path. That is, in this so-called

TABLE I. Comparison between the QM, QM_{ad}, and WKB calculations of the diagonal transitions.

Transition	$\alpha=0$		$\alpha=0.1$	
	QM	WKB	QM	QM_{ad}
$0\to0$	$1.67\cdot10^{-5}$	$1.60\cdot10^{-5}$	$1.40\cdot10^{-5}$	$1.40\cdot10^{-5}$
$2\to2$	$5.48\cdot10^{-13}$	$5.21\cdot10^{-13}$	$2.67\cdot10^{-13}$	$2.42\cdot10^{-13}$
$4\to4$	$1.44\cdot10^{-22}$	$1.34\cdot10^{-22}$	$4.66\cdot10^{-23}$	$3.62\cdot10^{-23}$

vibrationally adiabatic approximation (VA) one assumes that during the fission process the system always stays in the same oscillator state μ. Then one carries out a one dimensional calculation, taking into account only the change of the oscillator energy. Table I shows the diagonal-transition probabilities for no coupling ($\alpha = 0$) obtained with the exact quantum-mechanical program (QM) and with the one-dimensional WKB formula Eq. (3.1), and for a coupling $\alpha = 0.1$ obtained with the quantum-mechanical solution (QM) and for the adiabatic approximation (QM_{ad}). For this example it turns out that the adiabatic approximation is good.

For our model the inertial tensor is coordinate-independent and diagonal and therefore the methods described earlier, that is, the one-dimensional WKB approximation and the least-action-path method, give the same result and are independent of α. In Table I this result is also shown and is labelled WKB (and it is equivalent to the conserved-vibrational-energy, CVE, approximation). The reason why the results of the one-dimensional WKB method and the least-action-path method are independent of α is because they neglect the change of energy tied up in the motion perpendicular to the fission path (which may change during the tunneling).

The uniform semiclassical approximation

Now we will test the validity of the USCA (uniform semi-classical approximation) on this model problem. The underlying idea of the USCA is that one uses the analytical continuation of the classical equations of motion to describe the dynamics of the system together with quantized boundary conditions and the quantum-mechanical superposition principle in adding amplitudes for different trajectories. The foundations of the USCA and many applications to molecular scattering and reaction problems have been given by Miller and others (see Refs. 44, 45, and 46). Here we will therefore only give the main results of the USCA as applied to our model.

Let's introduce for the model problem in the asymptotic regions, that is for $|x| \to \infty$, the action-angle variables (J, q) for the transverse collective degree of freedom. The action variable J is related by the correspondence principle to the "quantum number" n of the harmonic oscillator through $J = 2\pi\hbar\,(n + \frac{1}{2})$ and the angle variable q to the phase ϕ of the oscillator through $q = \phi/2\pi$.

The semiclassical S-matrix, the square of which gives the transition probability between two quantum states $n_\mu \to n_\nu$, is given by[44]

$$S_{\nu\leftarrow\mu} = \sum \left(-2\pi i \left(\frac{\partial n_f(q_i)}{\partial q_i}\right)_{n_\mu}\right)^{-1/2} \exp[i\Phi(n_\nu, n_\mu)], \tag{29}$$

where the phase Φ is the classical action integral:

$$\Phi(n_\nu, n_\mu) = -\frac{1}{\hbar}\int_{t_i}^{t_f} (\dot{x}p_x + \dot{y}p_y)\,dt - \frac{1}{\hbar}(Jq - yp_y/2)\Big|_{t_i}^{t_f}. \tag{30}$$

The sum in Eq. (29) goes over all possible classical paths which satisfy the appropriate boundary conditions, that is, correspond to trajectories which tunnel through the barrier and are such that $n(t_i \to -\infty) = n_\mu$ and $n(t_f \to +\infty) = n_\nu$.

There are several differences between this USCA method and the two-dimensional method used by the Pauli group[18,30] which was described earlier. The main difference lies in the different boundary conditions used by the two methods. The way in which the boundary conditions are handled in the USCA method allows one to calculate penetrabilities from particular initial states (i.e., not only from the ground state but also from excited states) to particular final states. The USCA incorporates the full dynamics of the problem; that is, the energy tied up in the motion perpendicular to the fission path is included.

One way to proceed in order to find the paths with the correct boundary conditions is the following: Integrate the coupled classical Hamiltonian equations of motion starting from the left side at some distance $x = x_i$ (< 0) outside of the interaction region, with the collective oscillation in the quantum state n and with some arbitrary initial value of the angle variable q_i. The integration is directed so that tunneling is achieved and continued until $x = x_f$ (> 0) outside of the interaction region. The final "quantum number" n_f (usually not an integer) in which the transverse oscillatory degree of freedom is found is then a function of q_i. This way one finds the final quantum-number function $n_f(q_i)$. The classical paths which satisfy the correct boundary conditions are then those satisfying the equation

$$n_f(q_i) = n_\nu. \tag{31}$$

The way to obtain a trajectory that tunnels is to follow a time path in the complex time plane around the appropriate branch points.[45] This is most easily seen in the simple one-dimensional example of the barrier penetration through a symmetrical Eckard potential barrier.[46] This problem can be solved analytically, and the main results are summarized in Fig. 4. In the complex time plane the solution to this problem has pairs of branch points joined by cuts. If the time increments are kept real, then the particle is reflected at the barrier; if a purely imaginary time increment is chosen when the particle has reached the barrier, then the particle penetrates into the barrier. If one switched to real time increments again when the particle has reached the other side of the barrier, then the particle continues moving to the right and tunneling has been achieved.

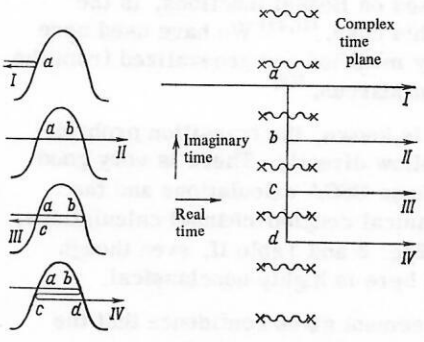

FIG. 4. Diagram showing on the right-hand side the different time paths one has to follow in order to obtain the trajectories shown on the left-hand side. The crosses represent the branch points and the wiggly line corresponds to the cuts joining them.

TABLE II. Comparison between the QM and USCA transition probabilities.

Method	$\alpha = 0.1$			
	$0 \to 0$	$0 \to 2$	$0 \to 4$	$2 \to 2$
QM	$1.40 \cdot 10^{-5}$	$9.30 \cdot 10^{-11}$	$1.03 \cdot 10^{-16}$	$2.67 \cdot 10^{-13}$
USCA	$1.44 \cdot 10^{-5}$	$9.49 \cdot 10^{-11}$	$0.97 \cdot 10^{-16}$	$2.52 \cdot 10^{-13}$
Method	$\alpha = 0.1$	$\alpha = 0.01$		
	$2 \to 4$	$0 \to 0$	$0 \to 2$	$0 \to 4$
QM	$9.86 \cdot 10^{-19}$	$1.64 \cdot 10^{-5}$	$1.22 \cdot 10^{-12}$	$1.49 \cdot 10^{-20}$
USCA	$9.15 \cdot 10^{-19}$	$1.56 \cdot 10^{-5}$	$1.30 \cdot 10^{-12}$	$1.42 \cdot 10^{-20}$

One has to proceed in essentially the same way in our two-dimensional example.

It is noted that in applying this semiclassical method one needs the analytical continuation of the equation of motion into the complex plane. For this to be possible one has to have an analytical expression for the potential energy in the Hamiltonian. A potential consisting of piecewise analytical functions cannot be continued analytically in a unique way into the complex plane, and therefore the USCA cannot be applied in this case. This, however, doesn't pose a major restriction to the method, since any potential-energy surface can be approximated in some way by an analytical function in the region of interest.

For our model we find that Eq. (31) has always two solutions; that is, there are two values of q_i (usually complex) that satisfy $n_f(q_i) = n_\nu$. The existence of complex initial and final phases causes no problems, since these phases are not observables. The quantities that are observables (for example, the initial and final quantum numbers n_μ and n_ν) are real in the asymptotic regions. In our calculation we have used $\alpha = 0.1$ and $\alpha = 0.01$, which correspond to small coupling, and therefore, as in the case of Coulomb excitation[48] and other cases studied,[47] we find that for the off-diagonal transitions only one of the two solutions of Eq. (27) contributes to the S-matrix (this may not necessarily be true for larger coupling constants). For the diagonal transitions, however, both roots contribute. Since the quantum-number function is very flat (because of the small coupling), a uniform semiclassical expression for the S-matrix, based on Bessel functions, is the appropriate one for this case.[47,49] We have used here an expression slightly modified and generalized from the one given by Stine and Marcus.[49]

Once the S-matrix is known, the transition probabilities $P_{\nu\leftarrow\mu} = |S_{\nu\leftarrow\mu}|^2$ follow directly. There is very good agreement between these USCA calculations and the exact quantum-mechanical coupled-channel calculations, as can be seen from Fig. 3 and Table II, even though the model considered here is highly nonclassical.

This very good agreement gives confidence that the semiclassical method may also be applied to more realistic cases with stronger coupling, where the numerical effort does not change very much and where a quantum-mechanical calculation would be unfeasible. Since coordinate-dependent inertial parameters introduce no additional difficulty, the USCA could be a useful tool to investigate the full dynamics of the coupling between the fission coordinate and the other degrees of freedom such as hexadecapole deformations, mass asymmetries, and change in pairing correlation.

3. THE COLLINEAR ATOM-DIATOMIC MOLECULE SYSTEM

Barrier penetration for a curving valley and nondiagonal mass tensor

Although this article is predominantly concerned with barrier problems in nuclear physics, it would leave a gap to fail to discuss also the two-dimensional barrier problem of great concern to theoretical chemists, the collinear collision of an atom such as hydrogen with a molecule H_2. The two common coordinates are x, the distance of the left-most atom from the central atom, and y, the distance of the right-most atom from the central atom. The Hamiltonian for relative motion, where we have constrained the center of mass to be at rest, is as follows:

$$H = m\dot{x}^2/3 + m\dot{x}\dot{y}/3 + m\dot{y}^2/3 + V(x, y). \tag{32}$$

Here m is the mass of a hydrogen atom, and $V(x, y)$ has the form of two valleys extending parallel to the respective coordinate axes and distant from them by the equilibrium bond distance of the H_2 molecule. The depth of the valleys in the asymptotic region is the bond energy of the molecule plus the zero-point vibrational energy. As one approaches the origin along the valleys, they rise to a saddle point at the energy of the linear symmetric "activated complex" for the exchange reaction of the central hydrogen atom. We note that with this choice of coordinates the inertial tensor is not diagonal. At the saddle point we may carry out a standard normal coordinate analysis by expanding the potential and retaining only the quadratic terms in the expansion.

$$V_{\text{saddle}}(x, y) = V_s + C_{xx}x^2/2 + C_{xy}xy + C_{yy}y^2/2, \tag{33}$$

where by symmetry the spring constant $C_{xx} = C_{yy}$ anywhere on the line $x = y$. Of the two eigenfrequencies of the determinantal equation one is real, ω_s, for the symmetric-stretch mode, and one imaginary, ω_a, for the asymmetric stretch mode. The normal coordinates lie along axes rotated by 45°, namely $(x + y)/\sqrt{2}$ and $(x - y)/\sqrt{2}$ for the symmetric and asymmetric stretch modes, respectively. This transformation can readily be seen by substitution, which diagonalizes both the mass tensor and the potential energy at the saddle. At any place along the line $x = y$, this transformation still removes the off-diagonal terms in the kinetic and potential energies, but a linear potential term in the symmetric-stretch coordinate is present everywhere except at the saddle.

Away from the line $x = y$, $C_{xx} \neq C_{yy}$, and the normal coordinate transformation, which eliminates the $\dot{x}\dot{y}$ and xy cross-terms, will involve a different coordinate transformation. In applying the vibrational adiabatic (VA) approximation to multidimensional barrier penetration with nondiagonal mass tensors, one needs to perform the normal coordinate transformation repeatedly along the tunneling trajectory in order to determine

the zero-point energy tied up in the modes orthogonal to the tunneling trajectory.

In one sense the collinear $H+H_2$ reaction problem is not ideal for understanding details of two-dimensional tunneling, since the problem has several complexities: the nondiagonal mass tensor, the curving valley, and a variable valley width (much broader at the saddle than in the asymptotic regions). However, such a great deal of numerical work is now available on the system that it affords the best illustrations of barrier penetrability in more than one dimension.

Truhlar and Kupperman[50] test two simple path-integral approximations against their full quantum-mechanical tunneling solutions. In both approximations the path is taken along the bottom of the potential valley, but in the CVE, conserved-vibrational-energy, approximation (similar to the previous spontaneous fission studies known to us) the potential-valley profile directly becomes the potential for a one-dimensional penetration calculation. In the VAZC, vibrationally adiabatic zero-curvature, approximation, one continuously alters the available energy in the tunneling path by subtraction of the zero-point energy of vibration at each point of the path. With the broader valley at saddle and lower zero-point energy, the VAZC leads to much greater penetrability than the CVE. The VAZC is in much better agreement with the quantum-mechanical calculations. However, for deeper tunneling the VAZC more and more underestimates tunneling, and this disagreement is attributed to the corner cutting inside the saddle. (In Appendix 1 we treat a simple model system of a curving valley to give insight into the corner-cutting phenomenon.)

In Sec. 2 we showed that by integration of classical equations of motion with complex variables (USCA) we obtained excellent agreement with quantum-mechanical coupled-channel calculations. The problem involved a straight valley of varying width. Our work was inspired largely by the work of George and Miller[45] on the $H+H_2$ problem. There is generally good agreement of their semiclassical work with the quantum-mechanical work, though Hornstein and Miller[51] have proposed some modifications to improve agreement over that shown in Duff and Truhlar's[52] paper. We show here in Fig. 5 the trajectory map of George and Miller,[45] nicely showing the corner cutting at two different energies. We would repeat the caution of these authors that they are plotting only the real part of complex coordinates, and that the particular time path of these calculations was not unique.

Even for vibrationally nonexcited cases one must use caution about the approach of finding a real least-action path and subtracting zero-point energy (VA) adiabatically for problems where the valley is curving or there are pecularities in the mass tensor. Such problems deserve to be studied fully quantum mechanically or by complex-trajectory USCA methods. At first glance it would seem that the two-dimensional tunneling path would originate at the classical turning contour. However, examination of the straight, constant-valley-width problem, which is exactly separable, makes evident that the tunneling trajectory must originate on a contour

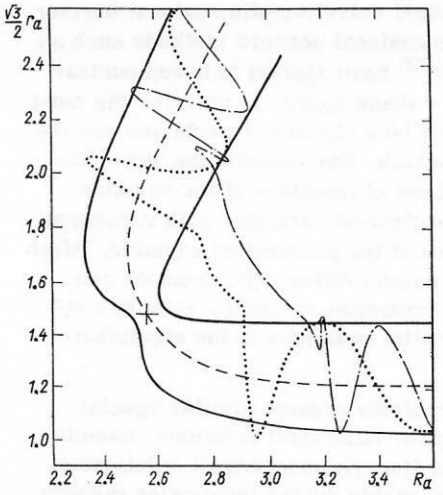

FIG. 5. Trajectories for reactive tunneling in the ground-state-to-ground-state $H+H_2$ reaction at a collision energy $E_0+0.20$ eV (dotted line) and $E_0-0.2$ eV (dash-dot line). For reference, the dashed line is the reaction coordinate, i.e., the path of minimum potential energy, and the cross is the saddle point. R_a and r_a are the real parts of the complex translational and vibrational coordinates, respectively. R_a and r_a are related to the coordinates x and y used in the text by $y=r_a$, $x=R_a-r_a/2$.

lower than the turning contour by the zero-point energy in the cross-valley direction. For tunneling close to the barrier top the simple WKB exponential penetrability is incorrect, and one should use the form of Fröman and Fröman[34]:

$$P_{VA}=\left\{1+\exp\left(\frac{2}{\hbar}\int_{x_A}^{x_B}\sqrt{2B_{xx}(V-E-\hbar\omega_y(x)/2)}\,dx\right)\right\}^{-1}, \qquad (34)$$

where the integral is taken along the least-action path, found by direct minimization or by solving classical equations of motion for the periodic orbit in imaginary time.

Another penetrability problem with curving trajectory comes from treating the pairing correlation as a collective coordinate as proposed by Moretto and Babinet[33] for spontaneous fission. In this case the least-action path is "pulled" off the valley floor by an inertial component B_{xx} that decreases with y (Δ). (Our example of Appendix 2 illustrates this "pulling" effect of a variable mass tensor.) This interesting problem deserves further treatment with realistic parameters and full two-dimensional dynamics.

4. OVERVIEW OF TWO-DIMENSIONAL BARRIER PROBLEMS

In addition to the exactly separable barrier problems, which reduce to one-dimensional penetration calculations, we have reviewed two classes of nonseparable problems. The case of alpha decay of spheroidal nuclei is characterized by channel-energy differences small compared to the total barrier height and kinetic energies far from the barrier. The cases of fission-barrier penetration and the collinear triatomic hydrogen reaction constitute a second class where the differences in channel energies are comparable to the barrier height and to the external total kinetic energies, with the question of closed channels also entering.

In principle one might solve two-dimensional barrier problems by two-dimensional network methods such as Kumar and Baranger[53] have applied to bound nuclear wave functions in β, γ shape space. In practice the most rigorous solutions for both classes of problems use the coupled-channel approach. One expands the wave function in an orthogonal set of functions of the variable cross-wise to the penetration variable, with expansion coefficients a function of the penetration variable. After substitution into the partial differential equation and integration over the crosswise variable, a set of coupled ordinary differential equations in the expansion amplitudes results.

Both classes of problems present similar special difficulties for computer numerical solutions, namely, only half of the set of linearly independent solutions of the wave equation are stable during integration through strong barriers. The exponentially decreasing solutions cannot be generated, since rounding errors in computation grow exponentially. One frequently has to impose double-ended boundary conditions by solving matrix equations based on the complete set of linearly independent solutions.

It is in the nature of the appropriate approximate methods that the two classes greatly differ. For the alpha-decay class with small channel-energy differences the Fröman—Nosov[9,14] matrix approximation is quite applicable. That is, one may construct a propagation matrix from solutions of the one-dimensional wave equation in the penetration variable carried out for fixed values of the other variable. The kinetic energy tied up in the crosswise motion (wave-function curvature) is not ignored but is handled in an averaged way.

For the class of fission and triatomic-hydrogen barrier problems the Fröman—Nosov approach is not valid. Often for this class of problems one is interested only in the penetrability of the nonvibrationally excited solution. In such situations it is appropriate to seek answers in terms of a one-dimensional WKB path integral along a path of least action. It is only recently that attention has been paid in the literature to the subleties of choice of path and the partition of available energy between the penetration mode and the other degree of freedom. The traditional choice of path at the bottom of the potential valley and over the saddle has been shown to be incorrect in cases where the valley curves. The least-action path cuts the corner more and more as the energy is dropped further below the saddle energy, thus giving an increased penetrability over that calculated by a path in the bottom of the valley. Moretto and Babinet[33] have shown how a variable mass tensor can also pull the least-action path away from the bottom of the valley.

Finally there is the question of partition of the kinetic energy between the two modes. The traditional approach is to neglect kinetic energy in the crosswise mode altogether. One stage better is to subtract the zero-point energy in the crossed mode from available energy for penetration. Truhlar and Kupperman[50] have shown for the triatomic hydrogen problem that this conserved vibrational (CVE) approxiation is not very good. In that problem the valley widens considerably at the saddle. They show that the vibrationally adiabatic (VA) approximation is much better; in the VA approximation the variable zero-point energy is subtracted at each point along the path when evaluating the one-dimensional WKB integral.

For problems in which vibrationally excited systems impinge upon the barrier there is as yet little experience with approximations. From coupled-channel solutions it would appear that there is generally a "vibrational-cooling" effect in transit of the barrier. That is, the exiting system is predominantly in the lowest vibrational zero-point state. Perhaps approximations to penetrability might be made by taking a product of the VA penetrability in the excited state in the region of sufficiently strong coupling and the VA penetrability in the zero-point state for the remainder of the barrier.

There are other more sophisticated approximate methods undergoing testing. In the semiclassical methods one integrates time-dependent classical equations of motion and by carrying the time path appropriately into the complex plane effects barrier penetration. It may be that these methods will prove more appropriate than coupled-channel methods for some cases, and they may furnish new physical insights into the problems. These methods appear to be more complicated for energies near the barrier top, where multiple paths contribute, and the application of the doubled-ended boundary conditions becomes much harder for more than two dimensions.

Recently attention has been focused on a method where one seeks a periodic orbit with time running in a purely imaginary direction. With imaginary time increments the kinetic-energy terms of the classical equations of motion reverse sign, and potential barriers invert into troughs. The approach is related to the more general semiclassical methods, except that here the variables (except time) may remain real. It remains to be proved whether one can properly incorporate motion in the crossed direction to bring in the full two-dimensional dynamics in this picture. Already this picture affords a useful way of thinking about multidimensional barrier penetration and the reciprocal behavior of positive and negative kinetic energy. As our examples in Appendices 1 and 2 illustrate, penetration paths cut inside the curving barriers by virtue of a negative centrifugal potential, while over-the-barrier trajectories are forced to the outside of the curving valley. Penetration paths of negative kinetic energy are pulled toward lower values of the penetration-mass-tensor component, while at positive kinetic energy the paths seek higher values of the tensor component. In a coupled-channel situation there is a vibrational-cooling effect for negative kinetic energies and a progressive exciting of vibrational modes for positive kinetic energies. We may reasonably surmise from the coupled-channel behavior that with inclusion of a friction term in the classical equations of motion we gain kinetic energy for tunneling paths, just as we lose kinetic energy to heat for increasingly fast real velocities.

The whole field of theoretical study of classically forbidden processes with more than one degree of freedom seems to be in a period of active development with

many open problems and a new plateau of deeper insight lying just ahead.

APPENDIX 1

Tunneling along a valley turning a corner

Both quantum-mechanical and semiclassical trajectory calculations on collinear $H + H_2$ reactive tunneling have shown that the deeper the tunneling the more the least-action path "cuts the corner". Thus, penetrability is systematically enhanced with curving valley over calculation following the valley floor. The numerical studies of the $H + H_2$ problem do not readily permit isolating effects due to curvature and effects due to valley widening at the saddle. Thus, it is of value to consider a model system of curving valley with constant width.

Consider a particle of mass μ, moving in a circular valley (see Fig. 6a) given by:

$$V(r) = (\hbar^2/2\mu)(A/r^2) + Cr^2/2 \tag{A1}$$

with $\sqrt{A} \gg 1$. The minimum of the valley occurs for

$$r_0 = \sqrt{\hbar/(\mu\omega)}\, A^{1/4} = aA^{1/4}, \tag{A2}$$

where $C = \mu\omega^2$ and $a \equiv \sqrt{\hbar/\mu\omega}$. One also has $V(r_0) = \sqrt{A}\hbar\omega$. The Schrödinger equation we have to solve is:

$$\left[-\frac{\hbar^2}{2\mu}\left(\frac{1}{r}\frac{\partial}{\partial r}\left(r\frac{\partial}{\partial r}\right) + \frac{1}{r^2}\frac{\partial^2}{\partial\varphi^2}\right) + \frac{\hbar^2 A}{2\mu r^2} + \frac{Cr^2}{2} - E\right]\Psi(r, \varphi) = 0. \tag{A3}$$

The solution to this equation is:

$$\Psi(r, \varphi) = \frac{1}{\sqrt{2\pi}} R_{nl}(r/a)\exp(il\varphi), \tag{A4}$$

where R_{nl} is solution of the radial equation:

$$\left[\frac{d^2}{d\rho^2} + \frac{1}{\rho}\frac{d}{d\rho} + \left(\frac{2E_{nl}}{\hbar\omega} - \rho^2 + \frac{l^2 + A}{\rho^2}\right)\right] R_{nl}(\rho) = 0. \tag{A5}$$

The solution of this equation has acceptable boundary conditions only when E_{nl} is given by:

$$E_{nl} = \hbar\omega(2n + 1 + \sqrt{A + l^2}) = E_{00} + E_{\text{ang}} + E_{\text{rad}} = \hbar\omega\sqrt{A} + \hbar\omega(2n + 1) + \hbar\omega(\sqrt{A + l^2} - \sqrt{A}), \tag{A6}$$

where n is an integer. The solution to Eq. (A5) can be expressed as[54]:

$$R_{nl}(\rho) = N_{nl}\exp(-\rho^2/2)\,\rho^{\sqrt{A+l^2}} L_n^{(\sqrt{A+l^2})}(\rho^2), \tag{A7}$$

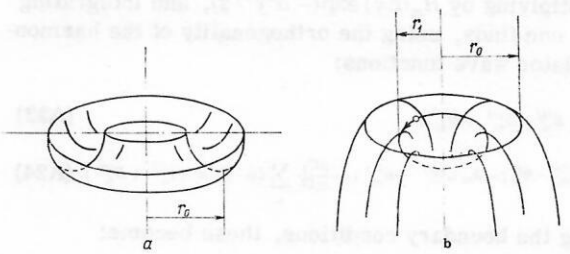

FIG. 6. A circular valley with the valley floor at r_0 is shown in a); if the potential shown in (a) is inverted one gets a circular hill as shown in (b).

where the Laguerre functions are defined by[55]:

$$L_n^{(\alpha)}(Z) \equiv \frac{e^Z Z^{-\alpha}}{n!}\frac{d^n}{dZ^n}(\exp(-Z)\, Z^{n+\alpha}).$$

A quantity measuring the average radial distance of a particle which moves around along the valley with angular momentum l and whose energy is E_{nl} is given by[54]

$$r_1 = \sqrt{\langle r^2\rangle} = \left[\int_0^\infty R_{nl}^2(r/a)\, r^3\, dr\right]^{1/2} = a(2n + 1 + \sqrt{A + l^2})^{1/2}. \tag{A8}$$

We want to study a tunneling process, that is, a case where the energy E_{ang} in the angular direction is negative. This is obtained when one takes imaginary l values (see Eq. (A6)): $l = il_0$ (l_0 real > 0). Let us also only consider the $n = 0$ case (for $n \neq 0$ the reasoning is similar). From Eq. (A4) one sees that the wave function for imaginary l is not a wave function corresponding to a stationary state, but to a state which is exponentially damped when the system tunnels around (angular part of the wavefunction is $\exp(-l_0\varphi)$). For r_1 we have then (assuming $\sqrt{A} \gg l_0$):

$$r_1 = a\sqrt{1 + \sqrt{A - l_0^2}} \approx a\sqrt[4]{A - l_0^2} \approx r_0(1 - l_0^2/A), \tag{A9}$$

i.e., we find that the particle moves more on the inner side with respect to the bottom of the valley; that is, in this "tunneling process" the system "cuts the corner".

The same result can also be understood from a more classical point of view, by finding the minimum $\bar{r}_1$ of the effective potential:

$$V_{\text{eff}} = V(r) + V_{\text{cent}}\ (r) = \frac{\hbar^2}{2\mu}\frac{A}{r^2} + \frac{1}{2}Cr^2 + \frac{\hbar^2}{2\mu}\frac{(il_0)^2}{r^2}; \tag{A10}$$

$$\bar{r}_1 = a\sqrt[4]{A - l_0^2}. \tag{A11}$$

The quantity $\bar{r}_1$ essentially agrees with r_1; that is, the minimum of the effective potential is further inside than the minimum of $V(r)$.

This ties in with the idea that the tunneling process can be understood by using classical equations of motion on the inverted potential. The problem becomes now to find the stable orbit of a system moving on a circular hill (with angular momentum l_0); see Fig. 6(b). The faster it moves, the more inside it must be. Equating the centrifugal force to the force exerted on the system by the potential (hill), we find:

$$\mathbf{f}_{\text{pot}} = -\frac{\partial V}{\partial r}\hat{r} = \left(Cr - \frac{\hbar^2}{\mu}\frac{A}{r^3}\right)\hat{r}; \quad \mathbf{f}_{\text{cent}} = \mu\frac{v^2}{r}\hat{r} = \frac{l^2}{\mu r^3}\hat{r};$$

$$\mathbf{f}_{\text{cent}} + \mathbf{f}_{\text{pot}} = \left(Cr - \frac{\hbar^2}{\mu}\frac{A}{r^3} + \frac{l_0^2}{\mu r^3}\right)\hat{r} = 0; \quad \bar{r}_1 = a\sqrt[4]{A - l_0^2}.$$

To summarize, for a system moving along a valley which turns a corner, for positive kinetic energies the centrifugal force pushes the system outwards (bobsled effect); for negative energies the centrifugal force is negative and during this tunneling process the system cuts the corner.

A quantity measuring the amount of corner cutting is $f=(r_0-r_1)/r_0$. Let us now express f in terms of C' (the "spring" constant of the circular valley), r_0 (the curvature of the valley turning a corner), and E_{ang} (the energy in the tunneling direction). We find

$$f=8\,|E_{\text{ang}}|/(C'r_0^2), \tag{A12}$$

with C' given by

$$C'=4\hbar^2A/(ar_1^2).$$

APPENDIX 2

Tunneling with variable mass along a straight valley

The potential we will consider is

$$V(x,\ y)=Cy^2/2, \tag{A13}$$

which represents a straight valley, the x axis being the valley floor. The mass tensor will be chosen diagonal but with a dependence on the y coordinate:

$$m_{xy}=m_{yx}=0;\quad m_{xx}=m_0(1+\alpha y/y_0);\quad m_{yy}=m_0, \tag{A14}$$

where $y_0=(\hbar^2/(m_0C))^{1/4}$. The parameter α is assumed to be small. From the classical Lagrangian one finds the following classical equations of motion:

$$\frac{d}{dt}\left[m_0(1+\alpha y/y_0)\,\dot{x}\right]=0; \tag{A15}$$

$$m_0\ddot{y}-\frac{1}{2}m_0\frac{\alpha}{y_0}\dot{x}^2+Cy=0. \tag{A16}$$

The first equation just gives the conservation of linear momentum in the x direction. We seek the straight-line trajectory along the valley for a tunneling case, that is, for the case where the kinetic energy in the x direction is negative. The straight-path trajectory has of course $\ddot{y}=\dot{y}=0$ and $y=\bar{y}=$ constant, $\bar{y}$ being the amount the straight track moves off the valley floor. From the equations of motion we find:

$$\bar{y}=\alpha m_0\dot{x}^2/(Cy_0).$$

Introducing the energy in the tunneling direction (which is negative), one finds

$$E_{\text{tun}}=(m_0/2)(1+\alpha\bar{y}/y_0)\,\dot{x}^2\approx\dot{x}^2m_0/2<0,$$

$$\bar{y}=-y_0\frac{\alpha}{2}\left(\frac{|E_{\text{tun}}|}{Cy_0^2/2}\right)=-\frac{\alpha\,|E_{\text{tun}}|}{Cy_0}. \tag{A17}$$

Essentially the same result is found when looking at the action integral and asking for what value of y it is a minimum; this occurs when

$$\frac{\partial}{\partial y}\sqrt{2m(1+\alpha y/y_0)(V-E)}=0$$

or

$$\frac{\partial}{\partial y}\left[\left(1+\alpha\frac{y}{y_0}\right)\left(\frac{1}{2}Cy^2-E\right)\right]\approx\frac{\partial}{\partial y}\left[\frac{1}{2}Cy^2-E-\frac{E\alpha y}{y_0}\right]=Cy-E\alpha/y_0=0.$$

We are considering the straight track, that is the case where there is no energy in the harmonic motion. The energy E is then the energy in the tunneling direction, $E=E_{\text{tun}}<0$. Using this, Eq. (A17) is readily found.

As a conclusion one can say that the trajectories for a tunneling process will shift toward the region of smaller inertia. The distance $\bar{y}$ which measures the distance between the equilibrium path and the floor of the potential energy depends on the important parameters of the problem in the way shown in Eq. (A17).

APPENDIX 3

Tunneling along a straight valley with variable valley width

The potential energy we will consider here is:

$$V(x,\ y)=[C_0+C_1\delta(x)]\,y^2/2. \tag{A18}$$

This corresponds to a straight valley (the x axis being the valley floor) whose width has a sudden jump at $x=0$. The mass tensor will be diagonal with constant elements equal to μ. The Schrödinger equation in this case is as follows:

$$\left[-\frac{\hbar^2}{2\mu}\left(\frac{\partial^2}{\partial x^2}+\frac{\partial^2}{\partial y^2}\right)+\frac{1}{2}[C_0+C_1\delta(\alpha x)]\,y^2-E\right]\Psi(x,\ y)=0. \tag{A19}$$

We want to consider a tunneling case along the valley; that is, the energy is to be negative. In both regions ($x\lessgtr 0$), the problem is separable, the wave function being:

$$\Psi=\sum_{n\geq 0}[A_n\exp(-k_nx)+B_n\exp(k_nx)]\,N_nH_n(\alpha y)\exp(\alpha^2y^2/2), \tag{A20}$$

where

$$k_n=[2\mu(\hbar\omega(n+1/2)-E)]^{1/2}/\hbar;\quad\alpha=(\mu\omega/\hbar)^{1/2},$$

with

$$\hbar\omega=\hbar\sqrt{C_0/\mu}.$$

We seek the solution with the boundary condition that at large negative x values only one particular vibrational state n_0 is incident ($A_n^{(l)}=\delta_{nn_0}$) and at large positive x values only decreasing waves are present ($B_n^{(r)}=0$). At the boundary $x=0$ the left and right wave functions have to join continuously; the delta function, however, introduces a discontinuity in the derivative, and we have:

$$\Psi^{(l)}(x=0,\ y)=\Psi^{(r)}\ (x=0,\ y); \tag{A21}$$

$$\frac{\partial}{\partial x}\Psi^{(l)}(x,\ y)\Big|_{x=0}=\frac{\partial}{\partial x}\Psi^{(r)}\ (x,\ y)\Big|_{x=0}-\frac{2\mu}{\hbar^2}\cdot\frac{C_1y^2}{2\alpha}\Psi(x=0,\ y). \tag{A22}$$

Substituting into (A21) and (A22) the expansion (A20), left multiplying by $H_m(\alpha y)\exp(-\alpha^2y^2/2)$, and integrating over y, one finds, using the orthogonality of the harmonic oscillator wave functions:

$$A_m^{(l)}+B_m^{(l)}=A_m^{(r)}+B_m^{(r)}; \tag{A23}$$

$$k_m(A_m^{(l)}-B_m^{(l)})=k_m(A_m^{(r)}-B_m^{(r)})+\frac{\mu C_1}{\alpha\hbar^2}\sum_n\langle m\,|\,y^2\,|\,n\rangle(A_n^{(r)}+B_n^{(r)}). \tag{A24}$$

Applying the boundary conditions, these become:

$$\delta_{mn_0}+B_m^{(l)}=A_m^{(r)}, \tag{A25}$$

$$\delta_{mn_0}-B_m^{(l)}=A_m^{(r)}+\frac{\mu C_1}{\alpha\hbar^2k_m}\sum_n\langle m\,|\,y^2\,|\,n\rangle A_n^{(r)}. \tag{A26}$$

We eliminate $B_m^{(1)}$ by adding

$$A_m^{(r)} + \frac{\mu C_1}{2\hbar^2 \alpha k_m} \sum_n \langle m | y^2 | n \rangle A_n^{(r)} = \delta_{mn_0}. \quad \text{(A27)}$$

The matrix elements are:

$$\langle m | y^2 | m \rangle = \frac{\hbar}{2\mu\omega}(2m+1);$$

$$\langle m | y^2 | m+2 \rangle = \frac{\hbar}{2\mu\omega}\sqrt{(m+1)(m+2)};$$

$$\langle m | y^2 | m-2 \rangle = \frac{\hbar}{2\mu\omega}\sqrt{m(m-1)}.$$

Consider the case of a nonexcited incident wave ($n_0 = 0$); one has:

$$A_0^{(r)} + \frac{\mu C_1}{2\hbar^2 k_0 \alpha} \frac{\hbar}{2\mu\omega} [A_0^{(r)} + \sqrt{2} A_2^{(r)}] = 1;$$

$$A_2^{(r)} + \frac{\mu C_1}{2\hbar^2 k_2 \alpha} \frac{\hbar}{2\mu\omega} [\sqrt{2} A_0^{(r)} + 5A_2^{(r)} + \sqrt{12} A_4^{(r)}] = 0;$$

These equations can be solved in a perturbation approach, if we assume that $C_1/(4\hbar\alpha\omega) = K < k_0$. Then we have the lowest order in the perturbation parameters K/k_n:

$$A_2^{(r)} \approx -\frac{K}{k_2}\sqrt{2}, A_0^{(r)} \simeq 1 - \frac{K}{k_0}$$

For the case of an incident wave with $n_0 = 2$, one finds similarly (to lowest order in the perturbation parameters):

$$A_0^{(r)} \approx \frac{K}{k_0}\sqrt{2}$$

$$A_2^{(r)} \approx \left(1 - \frac{K}{k_2}5\right)$$

$$A_4^{(r)} \approx -\frac{K}{k_4}\sqrt{12}$$

The $n = 0$ wave does not decay as fast as the $n = 2$ wave function, so at some distance $\bar{x}$ they will cross over and the $n = 0$ will dominate for larger distances. The distance $\bar{x}$ can be found from

$$A_0^{(r)} \exp(-k_0\bar{x}) = A_2^{(r)} \exp(-k_2\bar{x}).$$

[1]G. Breit and M.E. Ebel, Phys. Rev. **103**, 679 (1956); G. Breit and M.E. Ebel, Phys. Rev. **104**, B404 (1964).
[2]K. Alder *et al.*, Nucl. Phys. A **191**, 399 (1972).
[3]R.A. Broglia and Aa. Winther, Phys. Reports **4C**, 155 (1972).
[4]J.R. Oppenheimer, Phys. Rev. **31**, 349 (1928).
[5]M.C. Brinkman and H.A. Kramers, Proc. Acad. Sci. Amsterdam **33**, 973 (1930).
[6]G. Raisbeck and F. Yiou, Phys. Rev. **A4**, 1858 (1971).
[7]J.O. Rasmussen and B. Segall, Phys. Rev. **103**, 1298 (1956).
[8]G. Racah, Phys. Rev. **62**, 438 (1942).
[9]P.O. Fröman, Mat. Fys. Skr. Dan. Vid. Selsk. **1**, No. 3 (1957).
[10]J.O. Rasmussen and E.R. Hansen, Phys. Rev. **109**, 1656 (1958).
[11]S.G. Nilsson, Mat. Fys. Medd. Dan. Vid. Selsk., No. 16 (1955) (cf. Appendix A).
[12]E.M. Pennington and M.A. Preston, Canad. J. Phys. **36**, 944 (1958).
[13]A. Soinski, "Study of partial-wave branching in the alpha decay of ^{241}Am, ^{253}Es, and ^{255}Fm" (Ph.D. thesis, U. of Calif., Berkeley, 1974). LBL-3411.
[14]V.G. Nosov, Dokl. Akad. Nauk. SSSR **112**, 414 (1957) [Sov. Phys. Doklady **2**, 48 (1957)].
[15]V.M. Strutinsky, Zh. Éksp. Teor. Fiz. **32**, 1412 (1957) [Sov. Phys. JETP **5**, 1150 (1957)].
[16]R. Chasman and J.O. Rasmussen, Phys. Rev. **115**, 1257 (1959); Phys. Rev. **112**, 512 (1958).
[17]V.M. Strutinsky, Ark. Fys. **36**, 629 (1967); Nucl. Phys. A **95**, 420 (1967).
[18]M. Brack *et al.*, Rev. Mod. Phys. **44**, 320 (1972).
[19]S.G. Nilsson *et al.*, Nucl. Phys. A **131**, 1 (1969).
[20]V.M. Strutinsky and H.C. Pauli, Physics and Chemistry of Fission (Proc. Symp. Vienna, 1969), IAEA, Vienna, p. 155 (1969).
[21]M. Bolsteri *et al.*, Phys. Rev. C **5**, 1050 (1972).
[22]H.C. Pauli and T. Ledergerber, Nucl. Phys. A **175**, 545 (1971).
[23]P. Möller and J.R. Nix, Physics and Chemistry of Fission (Proc. Symp. Rochester, 1973), IEAE, Vienna, p. 103 (1974).
[24]M.G. Mustafa, U. Mosel, and H.W. Schmitt, Phys. Rev. C **7**, 1519 (1973).
[25]S.M. Polikanov *et al.*, Zh. Éksp. Teor. Fiz. **42**, 1464 (1962) [Sov. Phys. JETP **15**, 1016 (1962)].
[26]S.E. Larson and G. Leander, Physics and Chemistry of Fission (Proc. Symp. Rochester, 1973), IAEA, Vienna, p. 177 (1974).
[27]P. Möller and S.G. Nilsson, Phys. Lett. B **31**, 283 (1970); P. Möller, Nucl. Phys. A **192**, 529 (1972).
[28]J.R. Nix, Nucl. Phys. A **130**, 241 (1969).
[29]J. Damgaard *et al.*, Physics and Chemistry of Fission (Proc. Symp., Vienna, 1969), IAEA, Vienna, p. 213 (1969).
[30]T. Ledergerber and H.C. Pauli, Nucl. Phys. A **207**, 1 (1973).
[31]H. Hofmann and K. Dietrich, Nucl. Phys. A **165**, 1 (1971).
[32]H. Hofmann, Z. Phys. **250**, 14 (1972).
[33]L.G. Moretto and R.P. Babinet, Phys. Lett. B **49**, 147 (1974).
[34]P.O. Fröman and N. Fröman, JWKB Approximation, Contribution to the Theory (North Holland Press, Amsterdam, 1965).
[35]J. Randrup *et al.*, Nucl. Phys. A **217**, 221 (1973).
[36]J. Griffin, Proc. of Heavy Ion Summer Study, 1972, Oak Ridge, p. 123 (1972).
[37]L.D. Landau and E.M. Lifshitz, *Mechanics* (Pergamon, New York, 1972).
[38]H. Goldstein, *Classical Mechanics* (Addison-Wesley, Reading, Mass., 1950).
[39]J. Maruhn and W. Greiner, Phys. Lett. B **44**, 9 (1973).
[40]W.D. Meyers and W.J. Swiatecki, Ark. Phys. **36**, 343 (1967).
[41]W.H. Miller, J. Chem. Phys. **62**, 1899 (1975).
[42]H. Hofmann, Nucl. Phys. A **224**, 116 (1974).
[43]H. Massmann, P. Ring, and J.O. Rasmussen, Phys. Lett. B **57**, 417 (1975).
[44]W.H. Miller, J. Chem. Phys. **53**, 1949 (1970); **53**, 3578 (1970); W.H. Miller and T.F. George, J. Chem. Phys. **56**, 5668 (1972); J.D. Doll, T.F. George, and W.H. Miller, J. Chem. Phys. **58**, 1343 (1972).
[45]T.F. George and W.H. Miller, J. Chem. Phys. **57**, 2458 (1972).
[46]R.A. Marcus, J. Chem. Phys. **54**, 3965 (1972).
[47]W.H. Miller, Adv. Chem. Phys. **25**, 69 (1974); W.H. Miller, *The Classical S-matrix in Molecular Collisions*, in *Molecular Beams*, ed. K.P. Lawley, Wiley; to be published (1975).
[48]H. Massmann and J.O. Rasmussen, Nucl. Phys. A **243**, 155 (1975).
[49]J.R. Stine and R.A. Marcus, J. Chem. Phys. **59**, 5145 (1973).
[50]P.G. Truhlar and A. Kupperman, J. Chem. Phys. **56**, 2232 (1972).
[51]S.M. Hornstein and W.H. Miller, to be published, LBL-2595.
[52]J.W. Duff and D.G. Truhlar, Chem. Phys. Lett. **23**, 327 (1973).
[53]K. Kumar and M. Baranger, Nucl. Phys. A **92**, 608 (1967).
[54]W.H. Shaffer, Rev. Mod. Phys. **16**, 245 (1944).
[55]Jahnke-Emde-Losch, Tables of Higher Functions, McGraw-Hill, New York, 1960.

Translation edited by J.O. Rasmussen